Chronic G_q signaling in AgRP neurons does not cause obesity

Sedona N. Ewbank[a,b,1,2], Carlos A. Campos[a,b,1,2], Jane Y. Chen[a,b], Anna J. Bowen[a,b], Stephanie L. Padilla[a,b], Joseph L. Dempsey[c], Julia Yue Cui[c], and Richard D. Palmiter[a,b,1]

[a]Department of Biochemistry, University of Washington, Seattle, WA 98195; [b]Howard Hughes Medical Institute, University of Washington, Seattle, WA 98195; and [c]Department of Environmental and Occupational Health Sciences, University of Washington, Seattle, WA 98195

Contributed by Richard D. Palmiter, July 9, 2020 (sent for review March 16, 2020; reviewed by Roger A. Adan and Roger D. Cone)

Maintaining energy homeostasis requires coordinating physiology and behavior both on an acute timescale to adapt to rapid fluctuations in caloric intake and on a chronic timescale to regulate body composition. Hypothalamic agouti-related peptide (AgRP)-expressing neurons are acutely activated by caloric need, and this acute activation promotes increased food intake and decreased energy expenditure. On a longer timescale, AgRP neurons exhibit chronic hyperactivity under conditions of obesity and high dietary fat consumption, likely due to leptin resistance; however, the behavioral and metabolic effects of chronic AgRP neuronal hyperactivity remain unexplored. Here, we use chemogenetics to manipulate G_q signaling in AgRP neurons in mice to explore the hypothesis that chronic activation of AgRP neurons promotes obesity. Inducing chronic G_q signaling in AgRP neurons initially increased food intake and caused dramatic weight gain, in agreement with published data; however, food intake returned to baseline levels within 1 wk, and body weight returned to baseline levels within 60 d. Additionally, we found that, when mice had elevated body weight due to chronic G_q signaling in AgRP neurons, energy expenditure was not altered but adiposity and lipid metabolism were both increased, even under caloric restriction. These findings reveal that the metabolic and behavioral effects of chronic G_q signaling in AgRP neurons are distinct from the previously reported effects of acute G_q signaling and also of leptin insensitivity.

feeding behavior | hunger | adipose tissue | respiratory quotient

Energy homeostasis neural circuitry regulates how much adipose tissue an animal has by controlling feeding, thermogenesis, locomotion, and metabolism. Understanding how homeostatic systems are altered in obesity to support excess adiposity is essential for understanding and treating the disease.

Hypothalamic AgRP neurons are important for sensing energy needs and regulating energy intake and expenditure accordingly. During fasting, AgRP neurons are activated by ghrelin (1) and disinhibited by falling leptin levels (2). Activating AgRP neurons with chemogenetics or optogenetics increases food intake and decreases energy expenditure (EE) (3, 4). Conversely, AgRP neurons are rapidly inhibited following caloric intake by PYY and amylin and slowly inhibited by leptin (2, 5, 6). Chemogenetic inhibition of AgRP neurons suppresses food intake (3), and ablation of AgRP neurons leads to starvation (7).

In obese mice, AgRP neurons are chronically hyperactive (8). AgRP neurons in lean mice respond to leptin with decreases in firing rate, neuropeptide secretion, and STAT3 signaling, whereas AgRP neurons in obese mice are unresponsive to leptin by each of these measures (9, 10). The roles of hyperactivity and leptin resistance of AgRP neurons in obesity are unclear. Restoring leptin signaling in the arcuate nucleus in leptin-deficient rodents only partially corrects their obese phenotype (11, 12), but restoring leptin receptors selectively to AgRP neurons seems to fully correct the obese phenotype (13). Leptin receptor knockout restricted to AgRP neurons has been shown to cause either a modest (14) or robust (15) obese phenotype.

In the present study, we investigate the hypothesis that chronic excitation of AgRP neurons is sufficient to induce obesity. We chronically induce excitatory G_q signaling in AgRP neurons in mice using chemogenetics and characterize the resultant state through behavioral, electrophysiological, and metabolic experimentation.

Results

Chronic G_q Signaling in AgRP Neurons Is Not Sufficient to Maintain Chronic Elevation of Body Weight. Acute activation of AgRP neurons with the G_q-coupled designer receptor hM3Dq increases food intake and body weight (3, 16). We sought to determine whether prolonged chronic G_q signaling in AgRP neurons would support elevated body weight indefinitely. We virally transduced $Agrp^{Cre:GFP/+}$ mice with Cre-dependent, G_q-coupled designer receptor (hM3Dq:mCherry or with mCherry as a control) into the arcuate nucleus (Fig. 1 *A* and *B*) (17). We tested the efficacy of viral transduction of AgRP neurons by injecting clozapine-N-oxide (CNO) intraperitoneally (i.p.) and measuring subsequent food intake (Fig. 1*C*). Mice that ate less than 1 g in 4 h were excluded from experiments. To chronically activate the hM3Dq receptor in AgRP neurons, we added to the drinking water either CNO or clozapine (Clz, the active metabolite) (16, 18, 19). All mice had

Significance

Mammals maintain energy homeostasis and a stable body weight via neural circuits that regulate food intake and metabolism. Understanding how signaling within these circuits influences feeding, metabolism, and body weight is critical for understanding and treating diseases involving altered energy homeostasis, such as obesity and cachexia. Hypothalamic AgRP-expressing neurons are known to induce hyperphagia and decrease energy expenditure when acutely activated; however, the effects of chronic hyperactivity in AgRP neurons—which occurs in obese individuals—are unknown. Here, we show that chronic G_q-mediated activation of AgRP neurons in mice does not cause long-lasting obesogenic changes in feeding, body weight, gut microbiome, or energy expenditure, but does cause increased adiposity and increased lipid metabolism, even under caloric restriction.

Author contributions: S.N.E., C.A.C., and J. Y. Cui designed research; S.N.E., C.A.C., J. Y. Chen, A.J.B., S.L.P., and J.L.D. performed research; R.D.P. contributed new reagents/analytic tools; S.N.E. and J. Y. Chen analyzed data; S.N.E. wrote the paper; J.L.D. provided software; and R.D.P. provided resources, guidance, and editing.

Reviewers: R.A.A., University Medical Center Utrecht; and R.D.C., University of Michigan–Ann Arbor.

The authors declare no competing interest.

[1]To whom correspondence may be addressed. Email: snewbank@stanford.edu, camposca@uw.edu, or palmiter@uw.edu.

[2]S.N.E. and C.A.C. contributed equally to this work.

This article contains supporting information online at https://www.pnas.org/lookup/suppl/doi:10.1073/pnas.2004941117/-/DCSupplemental.

First published August 6, 2020.

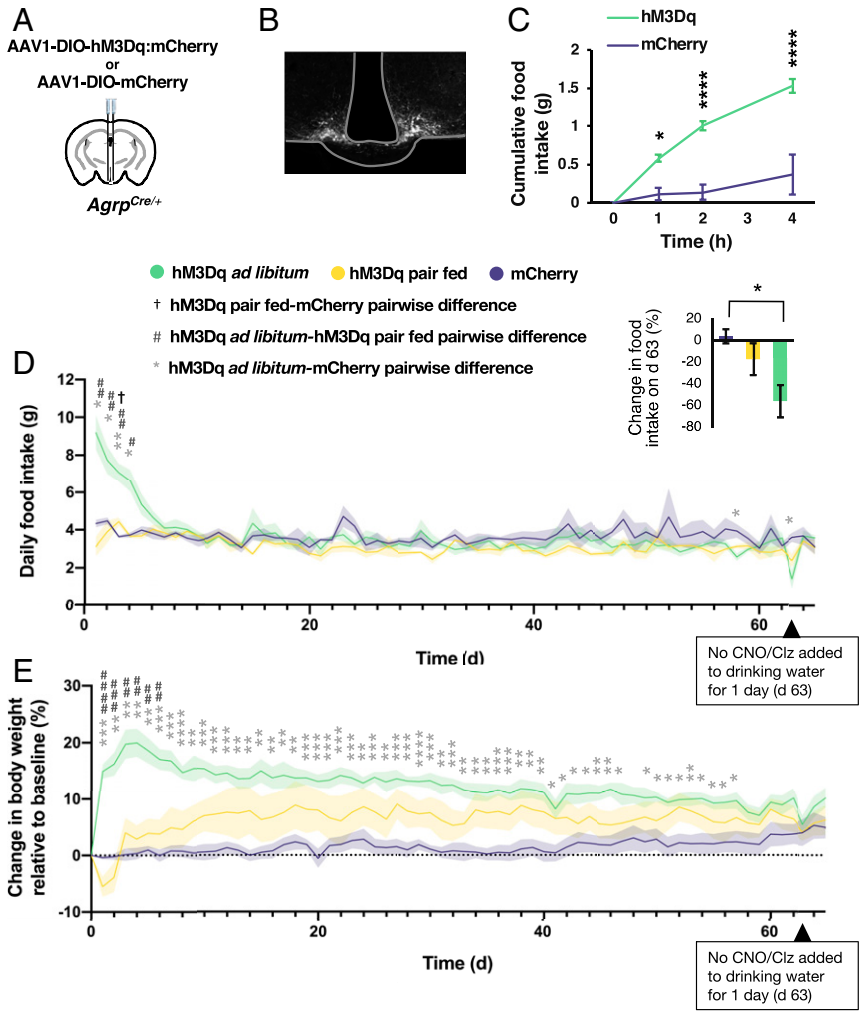

Fig. 1. Chronic G_q signaling in AgRP neurons is not sufficient to maintain chronic elevation of body weight. (*A*) Diagram of injection. (*B*) Histology of fluorescent AgRP neurons. (*C*) Food intake after CNO injection (two-way ANOVA; time: $F(1.986,27.80) = 34.27$, $P < 0.0001$; group: $F(1,14) = 29.50$, $P < 0.0001$; interaction: $F(3,42) = 13.67$, $P < 0.0001$; $^{*}P < 0.05$, $^{***}P < 0.001$, Sidak's multiple comparison). (*D*) Daily food intake during treatment with CNO (days 0 to 46) or Clz (days 47 to 62, and 64 and 65) in drinking water (mixed effects model; time: $F(6.556,83.690) = 8.638$, $P < 0.0001$; group: $F(2,13) = 1.847$, $P = 0.197$; interaction: $F(128,817) = 4.281$, $P < 0.0001$; $^{\dagger}P < 0.05$, $^{\#}P < 0.05$, $^{*}P < 0.05$, $^{\#\#}P < 0.01$, $^{**}P < 0.01$, Tukey's multiple comparison). (*Inset*) Change in daily food intake on day 63, when CNO/Clz treatment was not provided for 1 d, relative to average daily food intake across the 3 d immediately prior (one-way ANOVA: $F(2,13) = 6.432$, $P = 0.0114$; $^{*}P < 0.05$, Tukey's multiple comparison). (*E*) Body weight during CNO/Clz treatment (mixed effects model; time: $F(4.931,63.04) = 4.875$, $P = 0.0008$; group: $F(2,13) = 8.555$, $P = 0.0043$; interaction: $F(130,831) = 6.225$, $P < 0.0001$; $^{*}P < 0.05$, $^{\#\#}P < 0.01$, $^{**}P < 0.01$, $^{\#\#\#}P < 0.001$, $^{***}P < 0.001$, $^{\#\#\#\#}P < 0.0001$, $^{****}P < 0.0001$, Tukey's multiple comparison).

similar daily water intake (*SI Appendix*, Fig. S1*A*). To distinguish effects on weight caused by altered food intake, we included a group of hM3Dq-expressing mice that were pair-fed with controls and a group of hM3Dq-expressing mice fed ad libitum.

Chronic chemogenetic stimulation increased food intake in ad libitum-fed hM3Dq-expressing mice for the first 4 d, after which food intake did not differ significantly from controls (Fig. 1*D*). Surprisingly, hM3Dq-expressing mice that were pair-fed (i.e., food-restricted to match a control mouse's food intake) did not consistently consume all of the food provided to them (*SI Appendix*, Fig. S1*B*). Consequently, the average daily food intake of pair-fed hM3Dq-expressing mice was lower than that of controls on most days (Fig. 1*D*). Ad libitum-fed hM3Dq-expressing mice gained weight initially, but their weight gradually declined. Pair-fed hM3Dq-expressing mice lost weight initially while acclimating to food restriction but recovered and weighed more than controls but less than ad libitum-fed hM3Dq-expressing mice. By day 59, all groups had similar body weights (Fig. 1*E*).

To see whether chemogenetic stimulation was still influencing feeding behavior after 62 d of exposure, we stopped chemogenetic stimulation for 1 d. Removing chemogenetic stimulation resulted in hypophagia in ad libitum-fed and pair-fed hM3Dq-expressing mice, indicating that hM3Dq signaling was still effective (Fig. 1 *D*, *Inset*). Injecting CNO after prolonged chemogenetic stimulation did not increase feeding in ad libitum-fed hM3Dq-expressing mice, suggesting the CNO/Clz was already having a maximal effect (*SI Appendix*, Fig. S1*C*).

To further investigate how chronic stimulation of AgRP neurons affects feeding behavior, we used cages equipped with food-monitoring systems to study meal patterning. Mice expressing hM3Dq that were given 10 d of Clz treatment exhibited increased meal number (*SI Appendix*, Fig. S2*A*) and a small decrease in meal size, although this was not significant (*SI Appendix*, Fig. S2*B*). The hM3Dq-expressing mice receiving chronic Clz treatment responded normally to ghrelin or leptin injection (*SI Appendix*, Fig. S3),

suggesting that these signaling pathways were unaffected by chronic hM3Dq signaling.

AgRP Neurons Remain Sensitive to hM3Dq Receptor Activation and Receive Altered Presynaptic Input following Chronic Chemogenetic Stimulation. We considered the possibility that chronic activation of the hM3Dq receptor in AgRP neurons might promote down-regulation of chemogenetic signaling. To investigate this possibility, we used slice electrophysiology to record from hM3Dq-expressing AgRP neurons either in mice that had received 10 d of treatment with Clz in the drinking water or mice which had not been previously exposed to Clz. The hM3Dq-expressing AgRP neurons in Clz-treated mice had a lower baseline firing rate than hM3Dq-expressing AgRP neurons in untreated mice (4.4 ± 0.9 Hz for controls and 2.7 ± 0.5 Hz for 10-d Clz; Fig. 2 *A* and *B*), but bath perfusion of CNO elevated the firing rate to a similar frequency in both groups (7.2 ± 1.4 Hz for controls and 7.9 ± 1.5 Hz for 10-d Clz; Fig. 2*C*) such that the fold increase in firing rate was higher in the Clz-treated group (2.2 ± 0.4 Hz for controls and 3.6 ± 0.5 Hz for 10-d Clz; Fig. 2*D*). We thus conclude that 10 d of chronic Clz treatment did not desensitize AgRP neurons to chemogenetic induction of excitatory signaling by the hM3Dq receptor, in agreement with the behavioral data (Fig. 1*D*).

To investigate whether altered presynaptic input contributed to the decreased baseline firing rate of AgRP neurons in Clz-treated mice, we recorded spontaneous postsynaptic currents. We found that hM3Dq-expressing neurons in Clz-treated mice exhibited increased spontaneous inhibitory postsynaptic current (sIPSC) frequency (1.3 ± 0.3 Hz for controls and 2.8 ± 0.5 Hz for 10-d Clz; Fig. 2 *E* and *F*) but no changes in the amplitude of sIPSCs or the frequency or amplitude of spontaneous excitatory postsynaptic currents (sEPSCs; Fig. 2 *G*–*J*). This demonstrates that chronic chemogenetic stimulation of AgRP neurons evokes increased inhibitory presynaptic input, perhaps reflecting a network-level, negative feedback response.

Chronic G_q Signaling in AgRP Neurons Alters Nutrient Utilization but Not EE. Acute chemogenetic activation of AgRP neurons has been shown to alter metabolism by decreasing EE and increasing carbohydrate metabolism (3, 20). To study how chronic G_q signaling in AgRP neurons affects metabolism, we measured body composition, EE, and respiratory exchange ratio (RER) in mCherry-expressing and hM3Dq:mCherry-expressing mice (fed ad libitum or weight-matched with controls) prior to and following 10 d of chronic Clz treatment (Fig. 3*A*).

Ad libitum-fed hM3Dq-expressing mice gained body weight with chronic Clz treatment, accompanied by increased fat mass (Fig. 3*B*). Following chronic chemogenetic stimulation, hM3Dq-expressing mice that were weight-matched with controls also had increased fat mass and decreased lean mass (Fig. 3*B*).

Neither ad libitum-fed nor weight-matched hM3Dq-expressing mice had altered locomotion or EE during chronic Clz treatment (Fig. 3 *C* and *D*). Both ad libitum-fed and weight-matched hM3Dq-expressing mice exhibited decreased RER during the light cycle with chronic Clz treatment, indicating greater lipid metabolism (Fig. 3*E*). Thus, AgRP neuronal activation did not alter EE but did increase adiposity and fat oxidation, even during caloric restriction.

Chronic G_q Signaling in AgRP Neurons Does Not Alter Gut Microbial Ecology. Obese animals exhibit gut microbiome abnormalities that can influence lipid metabolism and EE (21–24). To determine whether inducing chronic G_q signaling in AgRP neurons alters the gut microbiota, we used 16S ribosomal RNA (rRNA) sequencing to profile the gut microbiota of mCherry- and hM3Dq:mCherry-expressing mice (fed ad libitum or pair-fed or weight-matched with controls) after 10 d of CNO treatment. We did not detect significant phylogenetic differences between the gut microbiota of any groups based on principal coordinate analysis of weighted UniFrac measures (Fig. 4 *A* and *B*) (25). All groups had similar microbial community diversity (Fig. 4*C*).

The obesity-associated gut microbiome has increased energy harvest capacity, as measured by fecal gross energy content (24). We found that fecal gross energy content of hM3Dq-expressing mice that had been treated with CNO for 28 d did not significantly differ from that of controls (Fig. 4*D*). These results indicate that chronic AgRP neuronal activation did not alter the gut microbiota or energy content of feces.

Discussion

We applied the excitatory designer receptor hM3Dq, which has been used extensively to investigate the behavioral and metabolic effects of AgRP neuronal activity (3, 16), to chronically introduce excitatory G_q signaling in AgRP neurons. We found that inducing chronic G_q signaling in AgRP neurons initially increases food intake and bodyweight, but food intake normalizes within a week, and body weight normalizes within 60 d.

We also provide electrophysiological evidence of a putative negative feedback response to chronic G_q signaling in AgRP neurons in the form of increased inhibitory presynaptic input (Fig. 2 *E* and *F*). It is plausible that the onset of this increased inhibitory input, which was measured following 10 d of chronic chemogenetic stimulation, may coincide with the decline of the initial hyperphagic response to chemogenetic stimulation (Fig. 1*D*). Circuit-tracing studies have shown that the primary sources of GABAergic modulation of AgRP neurons are presynaptic neurons in the arcuate and dorsal medial hypothalamic nuclei; thus, the neurons responsible for these sIPSCs likely reside in one of these brain regions (26). It is possible that the GABAergic neurons producing these sIPSCs may have increased activity or increased connectivity to AgRP neurons as a response to altered satiety signaling due to the increase in food intake and body weight initially produced by chemogenetic stimulation of AgRP neurons. Indeed, leptin signaling has been shown to increase inhibitory presynaptic input to AgRP neurons (27). Alternatively, the GABAergic neurons producing these sIPSCs could be downstream of AgRP neurons such that their increase in activity is a consequence of the increased activity of AgRP neurons, representing a true negative feedback neural circuit within the highly interconnected energy homeostasis neural circuitry.

Notably, mice can adapt behaviorally not only to chronic excitation of AgRP neurons but also to the loss of AgRP neurons; in both cases, the process takes about a week (28, 29). Ablation of AgRP neurons in adult mice leads to starvation, but various pharmacological or genetic interventions can prevent starvation and allow for restoration of normal feeding even after removal of the intervention (28, 29). The mechanisms underlying adaption to AgRP neuron ablation are unknown but presumably involve postsynaptic neurons and/or the circuits that they regulate. It is plausible that neurons and circuits involved in the process of adapting to AgRP neuronal ablation may also be involved in adaptation to the chronic stimulation of AgRP neurons described here. Future studies should be directed toward elucidating the circuits and signaling mechanisms involved in this adaptation process.

In our metabolic investigations, we demonstrate that inducing chronic G_q signaling in AgRP neurons for 14 d does not alter EE, but, paradoxically, increases adiposity while also decreasing RER. These effects occurred in both ad libitum-fed and food restricted animals, indicating that it is not a metabolic consequence of increased food intake or body weight but rather a more direct effect of AgRP neuronal activity. Acute chemogenetic activation of AgRP neurons has been shown to decrease EE and increase RER for several hours (3, 20); thus, our results reflect some longer timescale effect of chronic stimulation of AgRP neurons.

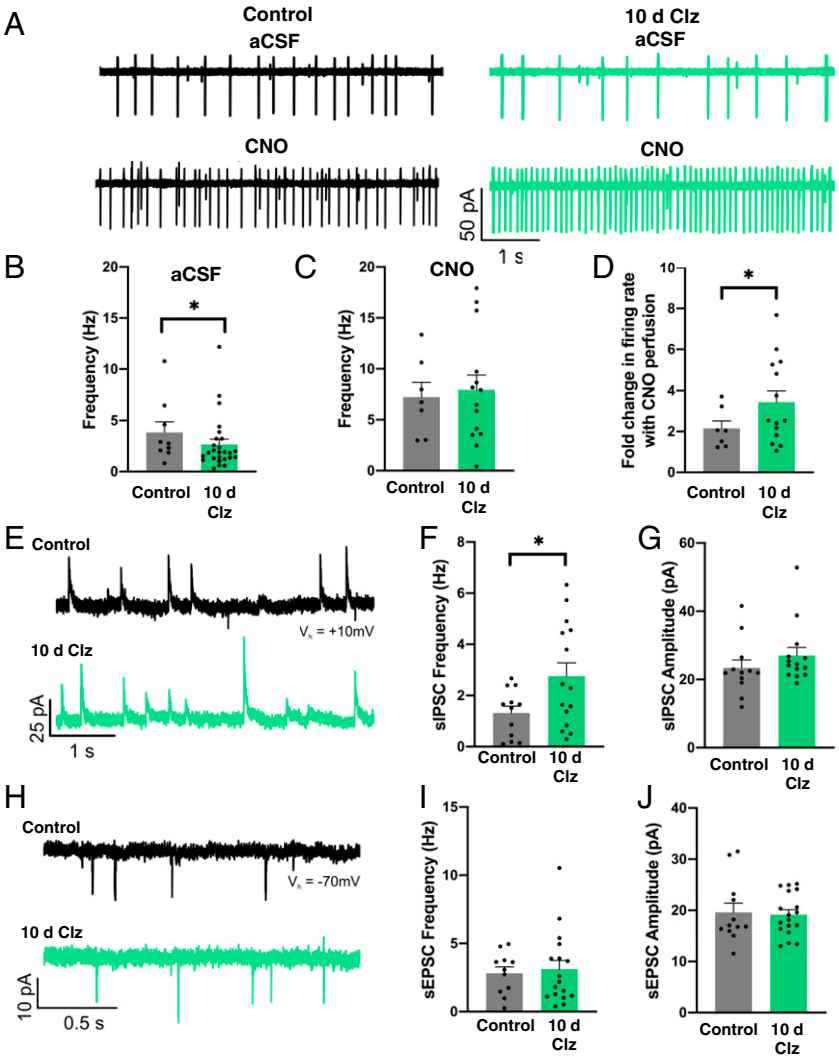

Fig. 2. AgRP neurons remain sensitive to hM3Dq receptor activation and receive altered presynaptic input following chronic chemogenetic stimulation. (*A*) Representative traces showing activity of hM3Dq-expressing AgRP neurons in artificial cerebrospinal fluid (aCSF) without any CNO (upper traces) or with 5 μM CNO (lower traces) in control (*Left*) and Clz-treated (*Right*) mice. (*B*) Firing rate of AgRP neurons in aCSF (control: 11 cells from six mice; Clz: 26 cells from five mice; Mann–Whitney Rank Sum Test: $U = 80.5$, $P = 0.039$; $^*P < 0.05$). (*C*) Firing rate of AgRP neurons in 5 μM CNO (control: seven cells from six mice; Clz: 14 cells from five mice; Student's *t* test: $t(19) = 0.305$, $P = 0.764$). (*D*) Fold change from baseline in CNO-evoked firing rate (control: nine cells from six mice; Clz: 14 cells from five mice; Student's *t* test: $t(21) = 2.289$, $P = 0.032$). (*E*) Representative sIPSC traces. (*F*) The sIPSC frequency (control: 12 cells from six mice; Clz: 15 cells from five mice; Welch's *t* test: $t(20.631) = -2.441$, $P = 0.024$; $^*P < 0.05$). (*G*) The sIPSC amplitude (control: 12 cells from six mice; Clz: 14 cells from five mice; Mann–Whitney Rank Sum Test: $U = 70$, $P = 0.487$). (*H*) Representative sEPSC traces. (*I*) The sEPSC frequency (control: 11 cells from six mice; Clz: 17 cells from five mice; Student's *t* test: $t(26) = 0.302$). (*J*) The sEPSC amplitude (control: 12 cells from six mice; Clz: 18 cells from five mice; Student's *t* test: $t(28) = -0.196$, $P = 0.846$).

The mechanism underlying these metabolic changes likely involves altered lipid and glucose synthesis and trafficking in the liver and adipose tissue. Chronic antagonism of melanocortin receptors (mirroring the pharmacology of AgRP signaling) increases glucose uptake and lipid synthesis in white adipose tissue while decreasing glucose uptake and thermogenesis in brown adipose tissue, leading to increased adiposity even with food restriction (30). Thus, the feeding-independent increase in adiposity could be due to increased adipocyte lipogenesis. We found it surprising that this increase in adiposity was accompanied by decreased RER, as this reflects increased size of lipid depots with a simultaneous increase in lipid utilization. A possible explanation is that, while fat mass is increased by chronic stimulation of AgRP neurons due to hyperphagia (in ad libitum-fed animals) and/or stimulation of lipogenesis, lipolysis could simultaneously be activated as part of a broader program of altered peripheral substrate utilization induced by chronic stimulation of AgRP neurons (31, 32). With this apparent simultaneous activation of lipogenesis and lipolysis, it is not clear whether mice that receive >60 d of chemogenetic stimulation of AgRP neurons and return to their baseline body weight would have normalized body composition or whether they would exhibit adiposity even at normal body weight, due to preferential storage of energy in adipose tissue.

Our findings have several important implications for understanding and treating chronic energy balance disorders. Others have shown that blunting leptin signaling in AgRP neurons (and thereby removing the inhibition and Janus tyrosine kinase/signal transducers and activators of transcription [JAK/STAT] intracellular signaling mediated by the leptin receptor) can cause sustained obesity (13, 15). We show that chronic excitatory G_q signaling in AgRP neurons with intact leptin signaling

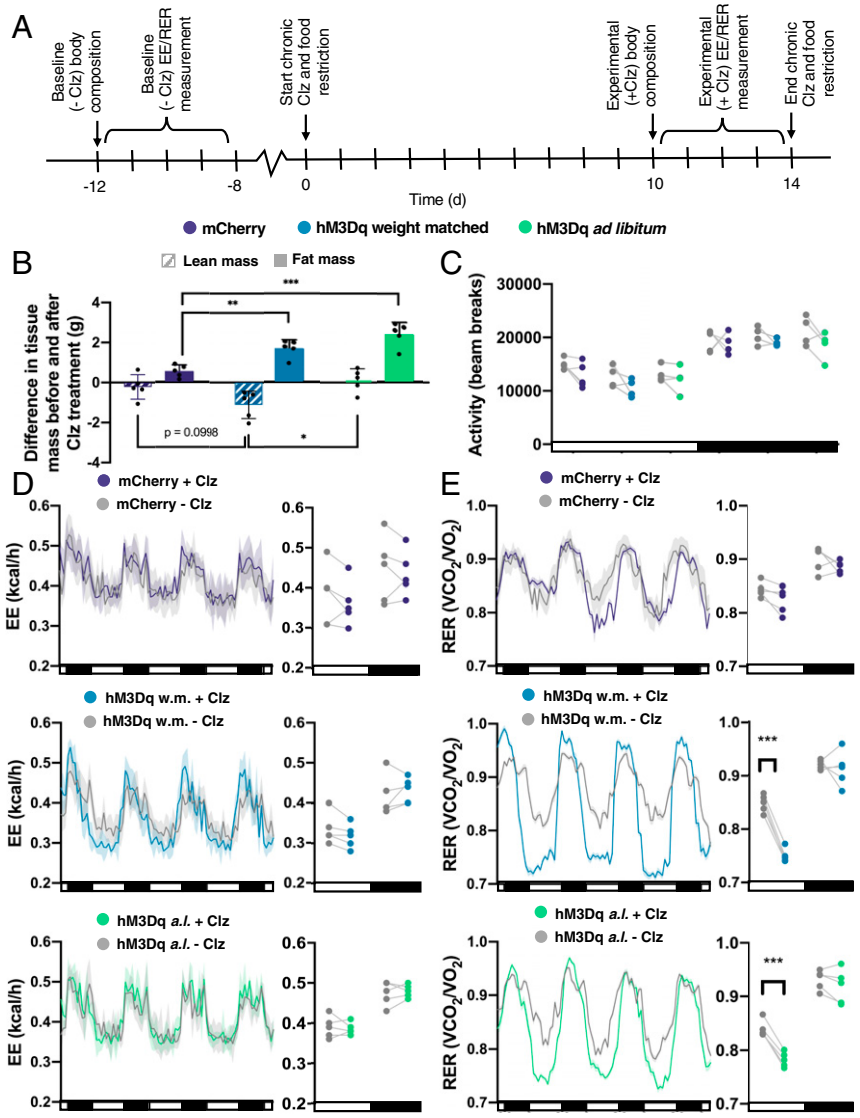

Fig. 3. Chronic G_q signaling in AgRP neurons alters nutrient utilization but not EE. (*A*) Experimental design schematic. (*B*) Change in lean and fat tissue mass after Clz treatment (lean one-way ANOVA: $F(2,12) = 5.120$, $P = 0.025$; Fat one-way ANOVA: $F(2,12) = 19.73$, $P = 0.0002$; $^*P < 0.05$, $^{**}P < 0.01$, $^{***}P < 0.001$, Tukey's multiple comparison). (*C*) Locomotion (all *t* tests had $P > 0.05$). (*D*) EE before and during Clz treatment, shown as a line graph (*Left*) and plotted points of averaged light (L) and dark (D) cycle measurements for each mouse (*Right*) (Student's *t* tests; mCherry: L: $t(8) = 0.478$, $P = 0.874$; D: $t(8) = 0.2224$, $P = 0.874$; hM3Dq weight-matched with controls (w.m.): L: $t(8) = 0.822$, $P = 0.681$; D: $t(8) = 0.534$, $P = 0.681$; hM3Dq ad libitum-fed (a.l.): L: $t(8) = 0.286$, $P = 0.910$; D: $t(8) = 0.399$, $P = 0.910$). (*E*) RER before and during Clz treatment, shown as a line graph (*Left*) and points (*Right*) (Student's *t* tests; mCherry: L: $t(8) = 1.604$, $P = 0.273$; D: $t(8) = 1.241$, $P = 0.273$; hM3Dq w.m.: L: $t(8) = 10.65$, $P < 0.0001$; D: $t(8) = 10.65$, $P = 0.604$; hM3Dq a.l.: L: $t(8) = 6.283$, $P = 0.0005$; D: $t(8) = 0.7475$, $P = 0.476$; $^{***}P < 0.001$).

(*SI Appendix*, Fig. S3 *C–E*) initially causes obesity, but is insufficient to sustain an obese state. Stated another way, both removal of JAK/STAT-coupled leptin signaling and chronic enhancement of G_q signaling can cause chronic hyperactivity of AgRP neurons; however, removal of JAK/STAT-coupled leptin signaling causes sustained obesity, whereas increased G_q signaling does not. This difference in results is likely due to differences between the JAK/STAT and G_q signaling pathways, and suggests that altered JAK/STAT signaling plays an important role in the obesogenic effects of suppressing leptin signaling in AgRP neurons. Additionally, our summary of the effects of chronic G_q signaling in AgRP neurons may be informative, given the robust interest in therapeutically targeting the melanocortin system for treating cachexia (33).

Materials and Methods

Animals. All procedures were approved by the University of Washington Institutional Animal Care and Use Committee. C57BL/6J $Agrp^{Cre:GFP/+}$ mice were bred and raised in a specific pathogen-free facility and fed standard chow (LabDiet 5053). The $Agrp^{Cre:GFP}$ knock-in mice (version 2) used in this study were generated by replacing the Cre:GFP cassette of the original line (34) with a new cassette designed to have attenuated expression of Cre:GFP. The new cassette differs from the original by 1) removing the nuclear localization signal from Cre, 2) using a nonoptimal initiation codon, 3) removing part of the N-terminal sequence of Cre, and 4) adding a 3′ untranslated region from the *Myc* gene that promotes a short messenger RNA half-life. The targeting construct was electroporated into G4 ES cells (C57BL/6 × 129/SV), and clones with correct targeting were identified by Southern blot of DNA digested with BamH1; 6 of 48 clones analyzed were correctly targeted. Three of these clones were injected into blastocysts from C57BL/6 mice, and one of them gave chimeras with a high percentage of

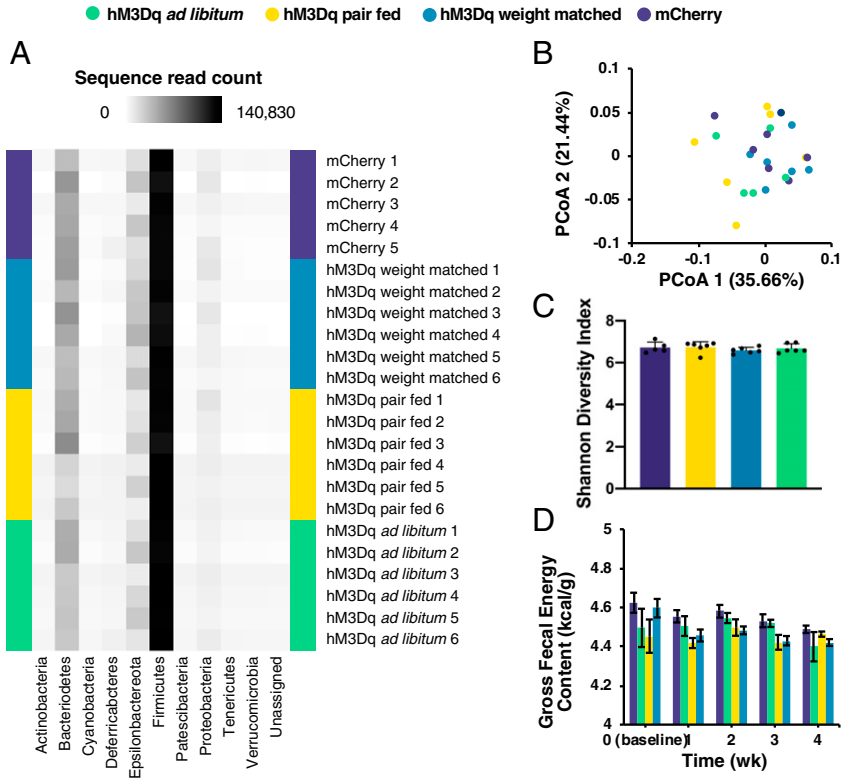

Fig. 4. Chronic G_q signaling in AgRP neurons does not alter gut microbial ecology. (*A*) Heat map of phyla abundance in gut bacteria of samples from individual mice after 10-d CNO treatment. (*B*) Principal coordinate analysis (PCoA) of weighted Unifrac metric in gut bacteria after CNO treatment (permutational multivariate analysis of variance: pseudo-$F(3,22) = 1.346$, $P = 0.182$). (*C*) Shannon index (sampling depth = 5,000; 10-iteration average; o-way ANOVA: group, $F(3,19) = 0.597$, $P = 0.625$). (*D*) Fecal gross energy content (two-way ANOVA: group, $F(3,12) = 1.902$, $P = 0.183$; time, $F(4,48) = 4.210$, $P = 0.005$; interaction, $F(12,48) = 0.924$, $P = 0.532$).

agouti color. Those chimeras were bred with *Gt(ROSA)26*^{FLPe} mice to remove the frt-flanked Neo gene. Thereafter, the mice were backcrossed to C57BL/6 mice for more than six generations before our experiments were performed. Crossing these mice with a conditional reporter line of mice (*Gt(ROSA)26*^{Ai14}, Allen Institute) gives faithful expression of tdTomato only in AgRP neurons, unlike the original line, which occasionally resulted in ectopic expression in many parts of the brain.

Surgery. Mice were anesthetized with 1 to 2% isoflurane in 0.8 L/min O_2 and positioned on a stereotaxic frame (David Kopf Instruments). Virus (490 nL per side) was bilaterally injected with a glass capillary attached to a nanoliter injector (Drummond Nanoject II) at −1.30 mm posterior to bregma, ±0.30 mm lateral to the midline, and −5.85 and −5.95 mm ventral to the surface of the dura. AAV1-Ef1a-DIO-hM3Dq:mCherry and AAV1-Ef1a-DIO-mCherry were produced as described (35).

Chemogenetics. For chronic chemogenetic stimulation, mice were given drinking water containing either 25 μg/mL CNO or 2.5 μg/mL clozapine (Clz, the active metabolite; Tocris 0444). CNO or Clz were dissolved in dimethyl sulfoxide (DMSO) before dilution in water; the final concentration of DMSO in water was 1.9 μL/mL or 0.27 μL/mL, respectively. Drinking water was replenished every 1 do to 3 d. For injections, CNO was injected i.p. at 1 mg/kg, 10 μL/g body weight during the light cycle.

Food Restriction. Pair-fed mice were given the amount of food consumed in the prior 24 h by a control mouse of a similar baseline body weight. Weight-matched mice were given an amount of food estimated to match their daily weight change to that of controls. Mice were fed, watered, and weighed within 2 h of dark-cycle onset.

Meal-Patterning Analysis and Hormone Treatment. Mice were habituated to cages fitted with a food-monitoring system (BioDAQ v.2.2) for ≥7 d before experimental manipulation. Feeding data were analyzed with BioDAQ Viewer v.2.2.01. A meal was defined as ≥0.06 g of food ingested with ≥300 s between meals (17). Ghrelin (2 mg/kg; Tocris #1465) and leptin (4 mg/kg; R&D Systems 398-LP) were dissolved in 0.9% saline and injected i.p. (10 μL/g body weight) in the last 20 min of the light cycle.

Slice Electrophysiology. Mice that were treated with Clz in the drinking water received treatment up until they were killed. Mice were intracardially perfused with 4 °C to 6 °C cutting solution containing (in millimolars) 92 *N*-methyl-D-glucamine, 2.5 KCl, 1.25 NaH_2PO_4, 30 $NaHCO_3$, 20 4-(2-hydroxyethyl)-1-piperazineethanesulfonic acid (HEPES), 25 D-glucose, 2 thiourea, 5 Na-ascorbate, 3 Na-pyruvate, 0.5 $CaCl_2$, 10 $MgSO_4$. Coronal slices (250 μm) were cut with a vibratome (Leica VT1200) and kept in the same cutting solution at 32 °C for 12 min. Slices were then placed in 25 °C aCSF containing (in millimolars) 126 NaCl, 2.5 KCl, 1.2 NaH_2PO_4, 18 $NaHCO_3$, 11 D-glucose, 2.4 $CaCl_2$, 1.2 $MgCl_2$. Recordings were made in aCSF continuously perfused at 32 °C. All solutions were continuously bubbled with 95%:5% O_2:CO_2 (pH 7.3 to 7.4, 300 mOsm to 310 mOsm). Patch-clamp recordings were obtained with a MultiClamp 700B amplifier (Molecular Devices) and filtered at 1 kHz. All recordings were taken with patch electrodes (3 MΩ to 5 MΩ) with an internal solution containing (in millimolars) 117 $CsMeSO_3$, 20 HEPES, 0.4 ethylene glycol-bis(2-aminoethylether)-*N*,*N*,*N*′,*N*′-tetraacetic acid, 2.8 NaCl, 5 tetraethylammonium, 4.92 Mg-ATP, 0.47 Na-GTP. Virally transduced AgRP neurons were identified by mCherry epifluorescence. Cells were held at V = −70 mV for recording EPSCs and at V = 10 mV for recording IPSCs. Postsynaptic-current recordings of 90 s were analyzed with an automated detection protocol in Mini Analysis Program v.6.0.7 (Synaptosoft) software and manually checked for accuracy. For recording CNO-evoked activity, cell-attached mode was used to record activity before and after 5 μM CNO in aCSF was perfused onto the tissue. After a slice was exposed to aCSF containing CNO, it was discarded. The 60-s baseline activity recordings and 60 s during CNO perfusion were analyzed in Clampfit v.11.0.3 (Molecular Devices).

Gut Microbiota Profiling. Mice were killed with Beuthanasia (i.p.), and cecal contents were isolated. Bacterial DNA was extracted from cecal extracts (E.Z.N.A. Stool DNA Kit, Omega Biotek). V4 of the bacterial 16S rRNA gene was PCR-amplified using 515F and 806R primers. Paired-end amplicon sequencing was performed with the Illumina MiSeq protocol (Beijing Genomics Institute). Forward- and reverse-sequence reads were denoised and merged with DADA2 (36). Taxonomy classification was performed with a Naïve Bayes classifier which was pretrained with the primers on the Silva 132 99% operational taxonomic unit database (37) in Quantitative Insights Into Microbial Ecology (QIIME) v.2.2018 (38).

Fecal Matter Bomb Calorimetry. Feces from 7 d were pooled for each mouse and desiccated at 60 °C for 48 h. Bomb calorimetry was performed with a plain jacket calorimeter (Parr 1341), digital calorimetric thermometer (Parr 6775), and oxygen bomb (Parr 1108). Data were analyzed in R v.3.3.1. The calorimeter system heat capacity was measured by cyclohexane combustion.

Body Composition Analysis. Fat and lean mass measures were determined by quantitative magnetic resonance spectroscopy (EchoMRI 3-in-1 Echo Medical Systems). The system was calibrated by scanning a known amount of fat in a calibration holder.

Indirect Calorimetry. Mice were placed in metabolic cages operated by the Energy Balance Core of the University of Washington Nutrition Obesity Research Center. EE measures were obtained with a computer-controlled indirect calorimetry system (Promethion, Sable Systems). Consecutive adjacent breaks in an XYZ beam array (BXYZ-R, Sable Systems) were scored as activity counts. Respiratory gases were measured as described (39). EE was calculated with the Weir equation (40). Data acquisition and processing were performed by MetaScreen v.2.3.12.4 and ExpeData v.1.9.14, respectively (Sable Systems).

Statistics. Statistics were computed in GraphPad Prism v.8.2.1. All error bars signify mean ± SEM.

Data Availability. All study data are included in the article and *SI Appendix*.

ACKNOWLEDGMENTS. We thank M. Chiang and S. Phelps for mouse husbandry; G. Stuber and M. Rossi for providing equipment, reagents, and advice for electrophysiology experiments; M. Schwartz, G. Morton, and all members of the R.D.P. laboratory for discussions; and K. Ogimoto and J. Nelson for metabolic experiments. This research was supported by funds from the Washington Research Foundation (to S.N.E.), Hope Funds for Cancer Research (to C.A.C.), and National Institutes of Health Grant R01-DA24908 (to R.D.P.).

1. M. Nakazato *et al*., A role for ghrelin in the central regulation of feeding. *Nature* **409**, 194–198 (2001).
2. K. A. Takahashi, R. D. Cone, Fasting induces a large, leptin-dependent increase in the intrinsic action potential frequency of orexigenic arcuate nucleus neuropeptide Y/Agouti-related protein neurons. *Endocrinology* **146**, 1043–1047 (2005).
3. M. J. Krashes *et al*., Rapid, reversible activation of AgRP neurons drives feeding behavior in mice. *J. Clin. Invest.* **121**, 1424–1428 (2011).
4. Y. Aponte, D. Atasoy, S. M. Sternson, AGRP neurons are sufficient to orchestrate feeding behavior rapidly and without training. *Nat. Neurosci.* **14**, 351–355 (2011).
5. L. R. Beutler *et al*., Dynamics of gut-brain communication underlying hunger. *Neuron* **96**, 461–475.e5 (2017).
6. Z. Su, A. L. Alhadeff, J. N. Betley, Nutritive, post-ingestive signals are the primary regulators of AgRP neuron activity. *Cell Rep.* **21**, 2724–2736 (2017).
7. S. Luquet, F. A. Perez, T. S. Hnasko, R. D. Palmiter, NPY/AgRP neurons are essential for feeding in adult mice but can be ablated in neonates. *Science* **310**, 683–685 (2005).
8. S. B. Baver *et al*., Leptin modulates the intrinsic excitability of AgRP/NPY neurons in the arcuate nucleus of the hypothalamus. *J. Neurosci.* **34**, 5486–5496 (2014).
9. P. J. Enriori *et al*., Diet-induced obesity causes severe but reversible leptin resistance in arcuate melanocortin neurons. *Cell Metab.* **5**, 181–194 (2007).
10. H. Münzberg, J. S. Flier, C. Bjørbaek, Region-specific leptin resistance within the hypothalamus of diet-induced obese mice. *Endocrinology* **145**, 4880–4889 (2004).
11. G. J. Morton *et al*., Arcuate nucleus-specific leptin receptor gene therapy attenuates the obesity phenotype of Koletsky (fa(k)/fa(k)) rats. *Endocrinology* **144**, 2016–2024 (2003).
12. R. Coppari *et al*., The hypothalamic arcuate nucleus: A key site for mediating leptin's effects on glucose homeostasis and locomotor activity. *Cell Metab.* **1**, 63–72 (2005).
13. A. M. Ramos-Lobo *et al*., Long-term consequences of the absence of leptin signaling in early life. *eLife* **8**, e40970 (2019).
14. E. van de Wall *et al*., Collective and individual functions of leptin receptor modulated neurons controlling metabolism and ingestion. *Endocrinology* **149**, 1773–1785 (2008).
15. J. Xu *et al*., Genetic identification of leptin neural circuits in energy and glucose homeostases. *Nature* **556**, 505–509 (2018).
16. S. L. Padilla *et al*., AgRP to Kiss1 neuron signaling links nutritional state and fertility. *Proc. Natl. Acad. Sci. U.S.A.* **114**, 2413–2418 (2017).
17. B. N. Armbruster, X. Li, M. H. Pausch, S. Herlitze, B. L. Roth, Evolving the lock to fit the key to create a family of G protein-coupled receptors potently activated by an inert ligand. *Proc. Natl. Acad. Sci. U.S.A.* **104**, 5163–5168 (2007).
18. J. L. Gomez *et al*., Chemogenetics revealed: DREADD occupancy and activation via converted clozapine. *Science* **357**, 503–507 (2017).
19. S. Jain *et al*., Chronic activation of a designer G(q)-coupled receptor improves β cell function. *J. Clin. Invest.* **123**, 1750–1762 (2013).
20. J. P. Cavalcanti-de-Albuquerque, J. Bober, M. R. Zimmer, M. O. Dietrich, Regulation of substrate utilization and adiposity by Agrp neurons. *Nat. Commun.* **10**, 311 (2019).
21. R. E. Ley *et al*., Obesity alters gut microbial ecology. *Proc. Natl. Acad. Sci. U.S.A.* **102**, 11070–11075 (2005).
22. P. J. Turnbaugh *et al*., A core gut microbiome in obese and lean twins. *Nature* **457**, 480–484 (2009).
23. F. Bäckhed *et al*., The gut microbiota as an environmental factor that regulates fat storage. *Proc. Natl. Acad. Sci. U.S.A.* **101**, 15718–15723 (2004).
24. P. J. Turnbaugh *et al*., An obesity-associated gut microbiome with increased capacity for energy harvest. *Nature* **444**, 1027–1031 (2006).
25. C. Lozupone, R. Knight, UniFrac: A new phylogenetic method for comparing microbial communities. *Appl. Environ. Microbiol.* **71**, 8228–8235 (2005).
26. A. S. Garfield *et al*., Dynamic GABAergic afferent modulation of AgRP neurons. *Nat. Neurosci.* **19**, 1628–1635 (2016).
27. S. Pinto *et al*., Rapid rewiring of arcuate nucleus feeding circuits by leptin. *Science* **304**, 110–115 (2004).
28. Q. Wu, M. P. Boyle, R. D. Palmiter, Loss of GABAergic signaling by AgRP neurons to the parabrachial nucleus leads to starvation. *Cell* **137**, 1225–1234 (2009).
29. Q. Wu, M. S. Clark, R. D. Palmiter, Deciphering a neuronal circuit that mediates appetite. *Nature* **483**, 594–597 (2012).
30. R. Nogueiras *et al*., The central melanocortin system directly controls peripheral lipid metabolism. *J. Clin. Invest.* **117**, 3475–3488 (2007).
31. A. Joly-Amado *et al*., The hypothalamic arcuate nucleus and the control of peripheral substrates. *Best Pract. Res. Clin. Endocrinol. Metab.* **28**, 725–737 (2014).
32. A. C. Könner *et al*., Insulin action in AgRP-expressing neurons is required for suppression of hepatic glucose production. *Cell Metab.* **5**, 438–449 (2007).
33. S. M. Krasnow, D. L. Marks, Neuropeptides in the pathophysiology and treatment of cachexia. *Curr. Opin. Support. Palliat. Care* **4**, 266–271 (2010).
34. E. Sanz *et al*., Fertility-regulating Kiss1 neurons arise from hypothalamic POMC-expressing progenitors. *J. Neurosci.* **35**, 5549–5556 (2015).
35. C. A. Campos, A. J. Bowen, M. W. Schwartz, R. D. Palmiter, Parabrachial CGRP neurons control meal termination. *Cell Metab.* **23**, 811–820 (2016).
36. B. J. Callahan *et al*., DADA2: High-resolution sample inference from Illumina amplicon data. *Nat. Methods* **13**, 581–583 (2016).
37. C. Quast *et al*., The SILVA ribosomal RNA gene database project: Improved data processing and web-based tools. *Nucleic Acids Res.* **41**, D590–D596 (2013).
38. J. G. Caporaso *et al*., QIIME allows analysis of high-throughput community sequencing data. *Nat. Methods* **7**, 335–336 (2010).
39. K. J. Kaiyala *et al*., Acutely decreased thermoregulatory energy expenditure or decreased activity energy expenditure both acutely reduce food intake in mice. *PLoS One* **7**, e41473 (2012).
40. J. B. Weir, New methods for calculating metabolic rate with special reference to protein metabolism. *J. Physiol.* **109**, 1–9 (1949).